

Model Esterification of Isophthalic and Terephthalic Acid with Benzyl Alcohol

AD W. M. BRAAM* and BOUDEWIJN J. R. SCHOLTENS

DSM Research, P.O. Box 18, 6160 MD Geleen, The Netherlands

SYNOPSIS

The esterification kinetics of isophthalic and terephthalic acid, with benzyl alcohol, were studied in the melt phase, which is a heterogeneous system because of the low solubilities of the phthalic acids. The relative concentrations of components and their conversions, α , were determined with HPLC. The effect of insolubility of the phthalic acids on the reaction kinetics can be described in two ways. For terephthalic acid, at $0 \leq \alpha \leq 1$, and for isophthalic acid, at $\alpha < 0.6$, the esterification kinetics can be described with equations for a homogeneous system with only a substitution effect. An improved and more complete description for isophthalic acid is obtained with equations for a heterogeneous system, with a surface reaction rate constant and a ratio of reactive (at the surface) over nonreactive monomers (in the core, i.e., the surface to volume ratio). This model fits data for $\alpha < 0.7$. The model parameters depend on the reaction temperature and the solubility of the phthalic acid. ©

1993 John Wiley & Sons, Inc.

INTRODUCTION

Polyesterification is an important condensation reaction, from both scientific and technological points of view. Usually, it occurs through an alternating copolymerization between multifunctional alcohols and carboxylic acids, via a stepwise intermolecular condensation of the functional groups. Such reactions can be described successfully with the stochastic theory of branching processes, originally developed by Flory and Stockmayer.¹⁻⁴ Later, Gordon et al.⁵⁻⁸ extended this theory to more complex systems, using probability generating functions and cascade substitutions as tools. In this way, substitution effects, insolubility and acidolysis, can be taken into account in an approximate way by combining this mean field theory with a set of differential equations that describe the kinetic effects.⁹⁻¹¹ This approach was recently employed to describe network formation in multistage processes,⁹⁻¹¹ which is of technological interest in many industrial production routes, for example, in the synthesis of resins for paints, coatings, adhesives, and construction ma-

terials. The verification of such theoretical models requires information on the reaction kinetics of the starting monomers. Recently, the reaction kinetics of two important multifunctional alcohols, namely neopentyl glycol and trimethylol propane, were studied with monofunctional 1,4-*tert*-butyl benzoic acid.¹²

This article describes the reaction kinetics of two commonly used dicarboxylic acids, namely terephthalic and isophthalic acid (TPA and IPA, respectively), with monofunctional benzyl alcohol (BA), in which they are only partly soluble at the start of the reaction. It is a direct continuation of a previous work,¹² with a similar experimental approach.

This study completes the experimental quantities required for describing the polyesterification of powder coating resins. The results obtained can be directly used in the theoretical model for such systems.^{10,11}

KINETIC EFFECTS DURING ESTERIFICATION

Since conversion, rather than time, is the variable of interest in our theoretical model,^{10,11} only sub-

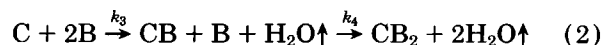
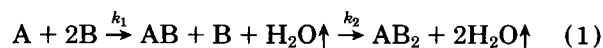
To whom correspondence should be addressed.

Journal of Applied Polymer Science, Vol. 50, 2007-2015 (1993)

© 1993 John Wiley & Sons, Inc.

CCC 0021-8995/93/112007-09

stitution and insolubility effects are to be determined and not the absolute reaction rate constants. The presentation and following discussion are condensed by assigning each reactant a single alphabetic letter (see Table I) and presenting the products with the combination of two reactant symbols. The reactions investigated are thus simply represented by:



where k_i represents the respective reaction rate constants. In the absence of substitution effects or insolubility, $k_1 = k_2$ and $k_3 = k_4$. The substitution effect parameter, $K_{AB} = k_2/k_1$ (or $K_{CB} = k_4/k_3$), represents the factor by which the reaction rate constant for monomer A, that is, k_2 (or C, i.e., k_4), which already reacted once with monomer B, is increased (K_{AB} or $K_{CB} > 1$, i.e., a positive substitution effect) or decreased (K_{AB} or $K_{CB} < 1$, i.e., a negative substitution effect) with respect to k_1 (or k_3).^{6-8,10-12}

Regardless of substitution effects, the conversions of TPA and IPA are given by

$$\alpha_A = (p_1 + 2p_2)/2 \quad (3)$$

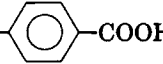
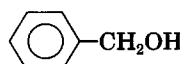
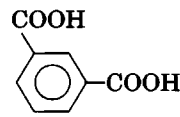
$$\alpha_C = (q_1 + 2q_2)/2 \quad (4)$$

respectively, where p_i and q_i represent the mole fractions of products (and starting monomers), carrying i ester groups. For random reactions between A and B, these mole fractions are given by the Bernoulli distribution:

$$p_i = \binom{2}{i} \alpha_A^i (1 - \alpha_A)^{2-i}, \quad i = 0, 1, 2. \quad (5)$$

The presence of kinetic effects is verified by com-

Table I Reaction Notation

Symbol	Chemical Name	Chemical Formula
A	Terephthalic Acid (TPA)	HOOC-  -COOH
B	Benzyl Alcohol (BA)	 -CH ₂ OH
C	Isophthalic Acid (IPA)	

paring experimental p_i (or q_i) data with the theoretical relations, presented in eq. (5). If systematic deviations occur, the value of the substitution effect parameter K is estimated with nonlinear regression analysis and a set of differential equations, presented in Appendix A, and called here *model 1*.

The low solubility of A and C is an important effect, which is expected to affect the overall reaction kinetics as measured experimentally. Insolubility can be handled artificially, with model 1 (by an artificial positive substitution effect), but the effect is more fully taken into account in *model 2*, and is described in more detail in Appendix A as well.

Model 2 contains three parameters to be determined by nonlinear regression analysis, namely the ratio ρ of reactive (at the surface) over nonreactive (in the core) monomers A (or C) at the beginning of the experiment (i.e., the initial surface to volume ratio), the ratio κ of the surface renewal rate constant over the esterification reaction rate constant, and the substitution parameter K (see Appendix A for details).

EXPERIMENTAL

Chemicals

Isophthalic acid was purchased from Janssen Chimica (> 99%), terephthalic acid was obtained from Amoco (fiber grade), and benzyl alcohol from Merck-Schuchardt Co. (synthetic grade). As a catalyst, a usual tin compound was used.¹² All chemicals were used as received, without further purification.

Reaction Vessel

The glass reaction vessel was approximately 0.5 l in capacity. A glass stirring rod was used for mixing at roughly 300 rpm. A Vigreux column, with a nitrogen purge at the top, was used to prevent the loss of benzyl alcohol, to create reaction conditions in the nitrogen atmosphere, and to allow the removal of excess water vapor produced during the reaction. The vessel was heated using a heating mantle, which was continuously regulated by a Coreci Microcor III with a "K-class" thermocouple, located in the reaction mixture. The reaction temperature was kept constant within $\pm 2^\circ\text{C}$.

Reaction Procedure

The total quantity of reactants was approximately 350 g. The materials were weighed to within 0.25%,

except for the catalyst, which was weighed to within 1.0%, due to the small quantities used (0.074% by mass compared to benzyl alcohol). The alcohol and acid were mixed in the reaction vessel under nitrogen atmosphere and were heated up to 150°C. The catalyst was then added and the reaction vessel was heated up to the reaction temperature within several minutes. From the moment the reaction temperature was reached, samples of approximately 0.3 g were taken at regular time intervals. To prevent reactions in the samples taken, and to prepare these for the HPLC analysis, the samples were poured into excess acetonitrile. Typically, 10 to 20 samples were taken during a reaction run. The reaction time depended on the reaction temperature and catalyst concentration, and essentially varied from 5 to 30 h to obtain 80% conversion.

HPLC

The composition of samples, taken from the reaction mixture, was determined with High Performance Liquid Chromatography. The HPLC included a Philips PU 8270 UV/VIS spectrophotometer, an HP

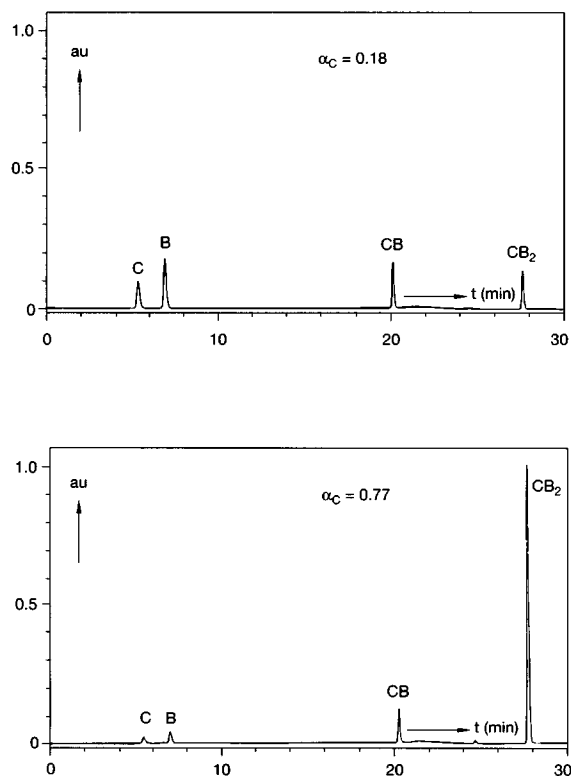


Figure 1 Typical HPLC chromatograms for IPA; (upper part) at low conversion, (lower part) at high conversion.

Table II Absorption Sensitivities Used in HPLC

Compound	Wavelength (nm)	Sensitivity, c_i ($s \text{ mol}^{-1}$)	Standard Deviation in Sensitivity (σ_{c_i})
B	245	391	2
A	245	0.00516	0.00005
AB	245	2.046	0.004
AB ₂	245	1.740	0.003
B	210	5.811	0.011
C	210	1.065	0.007
CB	210	0.911	0.005
CB ₂	210	0.716	0.004

Note: Sensitivities c_i are a result of: $A_x = c_x X$, in which X = amount of component x ($x = A, AB, \text{etc.}$, in mol) analyzed, and A_x = area of the corresponding HPLC peak (in s).

1090 PV5 solvent delivery system, a Spark Promis automatic sample injector ($5 \mu\text{L}$), a 250×4 mm column of Nucleosil C₁₈, and a diode array detector. The eluent was a mixture of acetonitrile and 0.01 M phosphoric acid, changing in composition during a run from 22/78 (vol %/vol %) initially to 5/95 after 28 min. This gradient affected baseline separation clearly and the nonoverlapping of peaks when operated at room temperature and at an eluent flow of 10 mL/min. Peak integration was computer-assisted. Two typical HPLC chromatograms, related to reaction (2), are shown in Figure 1.

Calibration curves for absorption sensitivities of B, A, AB, and AB₂ were determined experimentally at 245 nm and of B, C, CB, and CB₂ at 210 nm. The mono- and diesters were purified by repeated dissolution in acetonitrile and precipitation in water. The sensitivities, so obtained, are presented in Table II.

From the HPLC data (peak areas with an accuracy of 1.5%), the ratios $[AB]/[B]$, $[AB_2]/[B]$, $[CB]/[B]$, and $[CB_2]/[B]$ were determined; $[A]/[B]$ and $[C]/[B]$ were neglected due to non-representative sampling of these heterogeneous systems. As analysis of the distillate showed no significant loss of benzyl alcohol, the system was considered to be closed. From the respective mass balances $[A]$, $[C]$, and $[B]$ were obtained (see Appendix B), and from all these data the respective reaction states and conversions were obtained.

Solubility

The solubilities of the phthalic acids in benzyl alcohol at 200°C were determined from HPLC data

Table III Solubilities in Benzyl Alcohol at 200°C

Acid	Solubility (g acid/100 g Solution)	Standard Deviation in Solubility
A	1.4	0.6
C	8.9	0.7

of saturated solutions. The results are collected in Table III.

RESULTS AND DISCUSSION

The esterification reactions are carried out in bulk under nonideal conditions. During initial heating (from 150°C to the final reaction temperature) and sampling, the reaction kinetics may be influenced, so that uncertainty in reaction time is larger than in conversion. By determination of conversion through sampling, errors can be introduced, due to unknown reactions during cooling of the sample. However, the residence time of a sample between experimental conditions and dilution with acetonitrile is small enough, with respect to reaction times in the bulk, to justify the neglect of such errors. Corrections are made for the loss of benzyl alcohol (if any) by linear interpolation of this loss between $\alpha = 0.0$ and α_{\max} .

From these experimental data, the appropriate values of p_i , q_i , α_A , α_C , and their standard deviations, are obtained. These data sets already contain qualitative information about substitution effects, as demonstrated in Figure 2, which contains curves of

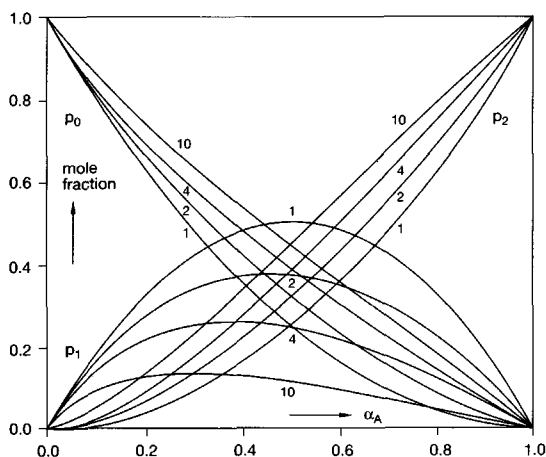


Figure 2 Theoretical reaction state for a 2-functional monomer A for several values of K .

the fractions of mono-, di-, and trimers of A, calculated for various values of a positive substitution effect.

To obtain values of the model parameters, a non-linear regression is carried out. The quality of the regression is described by the Goodness of Fit:

$$\text{GoF} = \sqrt{\sum_{i=1}^{N_o} \frac{w_i e_i^2}{N_o - N_v}} \quad (6)$$

in which $w_i = (\text{standard deviation})^{-2}$, $e_i = \text{deviation between experimental and calculated value}$, $N_o = \text{number of observed data points } i$, and $N_v = \text{number of independent variables}$.

In *model 1*, all kinetic and insolubility effects are

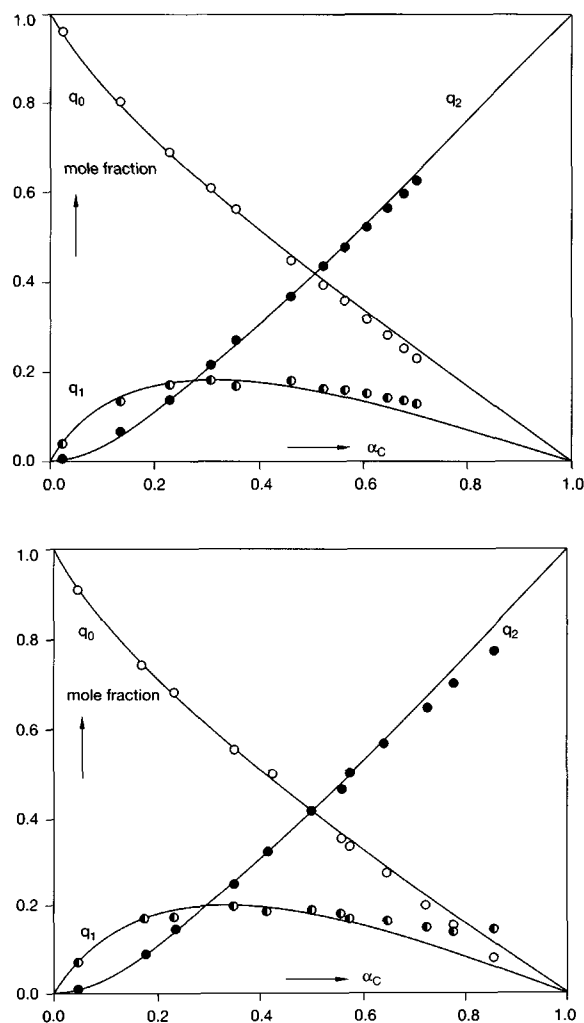


Figure 3 Experimental (two combined runs) and fitted reaction states of IPA at 200°C (model 1). (a) Curve calculated with $K = 6.60$ and (b) curve calculated with $K = 5.68$.

taken into account by a single substitution parameter K . In Figure 3, some typical results are presented for reaction (2) at 200°C. As can be seen in Figure 3, the fit is good for $\alpha < 0.6$, but systematic deviations between calculated and observed data are found for $\alpha > 0.6$.

The substitution parameter obtained with model 1, which we ascribe primarily to the low solubility of the phthalic acids, appears to be dependent on the reaction temperature (see Table IV and Fig. 4). At low temperatures, k_3 is slowed down relative to k_4 , that is, K_{CB} increases [see reaction (2)]. This can be easily understood from a reduction in solubility at lower temperatures. From this it can also be concluded that a small change in reaction temperature will immediately affect the value of K . Thus, the significant differences between K_{CB} from duplo experiments (at 200°C, see Table IV), can be assigned to different experimental conditions and are not the result of the regression analysis.

The lower solubility of TPA (see Table III) leads as a consequence to a small amount of reactive p_0 and p_1 (see Fig. 5). This implies, in model 1, that the effective $k_1 \ll k_2$, corresponding to a strongly positive substitution effect and a large value for K_{AB} (see Table IV). It is interesting to note that the reaction kinetics of such heavily heterogeneous systems, such as those studied here, can yet be described by equations based on homogeneous systems with only a substitution effect.

In model 2, which was developed to improve the fit in particular at high conversions, the presence of undissolved particles is explicitly taken into account. In principle, this implies that both chemical effects (K), and physical effects (κ , ρ), can be described simultaneously. However, simultaneous parameterization of K , κ , and ρ was usually impossible, due to strong correlations (see Table V). This implies that different sets of K , κ , and ρ result in fits of equal quality. Thus, the chemical physical background of

Table IV Substitution Effect Parameters Derived from Model 1 for Various Reaction Conditions

Acid	Temperature (°C)	K	σ_K	GoF
C	160	11.99	0.08	5.7
C	180	8.78	0.06	2.5
C	190	6.98	0.06	2.9
C	200	6.60	0.07	2.4
C	200	5.68	0.07	2.4
A	200	49.8	0.3	4.2

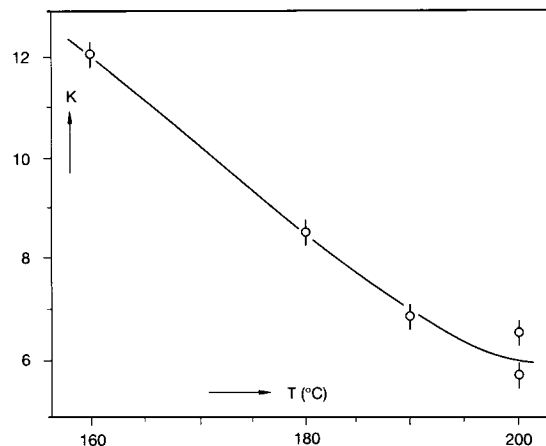


Figure 4 Substitution parameter K of IPA as a function of temperature (model 1).

the equations used (see Appendix A) show so many similarities that the individual contributions cannot be separated.

As a counterpart to model 1, all kinetic effects can be described in terms of completely insoluble phthalic acid, which only reacts at the particle surfaces ($K = 1$ and κ and ρ are the model parameters), which is a special case of model 2. The results, so obtained, are collected in Table VI and Figures 6 and 7. Note that the experimental results are identical to those in Figures 3 and 5.

The essence of model 2 is that the first reaction of the only slightly soluble monomer is merely described as a reaction at the surface, which is subsequently renewed by diffusion of the dimers into

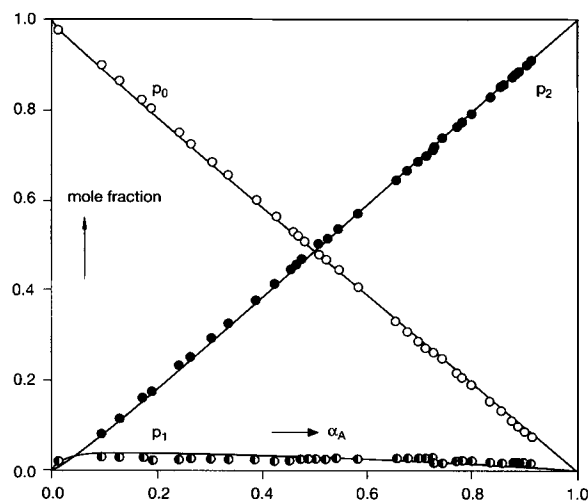


Figure 5 Experimental and fitted reaction states of TPA at 200°C (model 1). Curve calculated with $K = 49.8$.

Table V Normalized Variance–Covariance Matrix for Reaction (2) at 200°C

	K	κ	ρ
K	1.0	0.9997	0.9954
κ	0.9997	1.0	0.9941
ρ	0.9954	0.9941	1.0

the melt. As can be seen from the regression results of IPA, this description works well for $\alpha < 0.7$.

By comparing Figures 3 and 6, it can be seen that the parameterized description of the reaction states of IPA is improved in model 2, although systematic deviations between calculated and observed data still occur at $\alpha > 0.7$. The improvement of the description can also be demonstrated by comparing the GoFs of Tables IV and VI. From Figures 5 and 7, and Tables IV and VI, it can be concluded that only minor differences occur in the description of the reaction states of TPA with both models.

The influence of the temperature on the reaction kinetics of IPA in model 2 is shown in Figure 8. The surface to core ratio (ρ) is essentially insensitive to the reaction temperature, whereas κ , which is the ratio of the surface renewal rate constant, k_s , over the esterification rate constant, k_3 , strongly increases with increasing temperature. Thus k_s increases more strongly with temperature than k_3 .

The independence of the surface to core ratio (ρ) to the temperature is not so surprising for insoluble particles. However, as IPA is not completely insoluble, the value of p_o' (and ρ) also should reflect its partial solubility. Because the model parameters κ and ρ are still, to some extent, dependent (coupled, see Table VI), the interpretation of the individual dependences on temperature is not completely correct. Nevertheless, the strong temperature dependence of κ , and the apparent independence of ρ , suggest that the kinetic effect (dissolution rate of once reacted monomers) is more

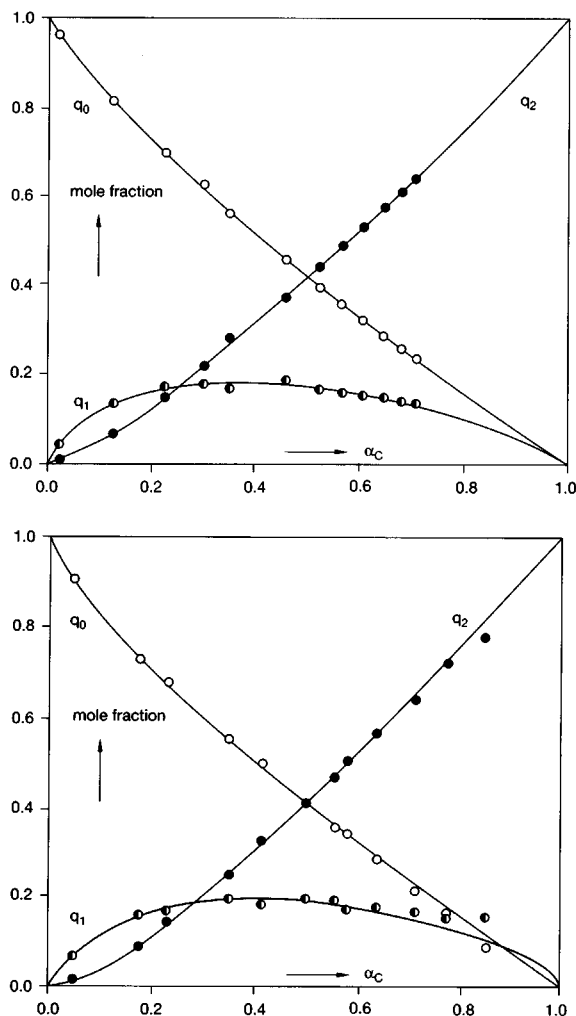


Figure 6 Experimental (two combined runs) and fitted reaction states of IPA at 200°C (model 2). (a) Curve calculated with $\kappa = 1.69$ and $\rho = 0.097$ and (b) curve calculated with $\kappa = 1.98$ and $\rho = 0.128$.

temperature dependent than the thermodynamic equilibrium (i.e., solubility).

The lower solubility of TPA at 200°C, in com-

Table VI Substitution Effect Parameters Derived from Model 2 for Various Reaction Conditions (K Fixed at 1.0)

Acid	Temperature (°C)	κ	σ_x	ρ	σ_ρ	Correlation Coefficient	GoF
C	160	0.28	0.003	0.115	0.003	-0.43	5.6
C	180	0.39	0.003	0.070	0.003	-0.19	1.2
C	190	0.50	0.005	0.097	0.005	-0.21	1.9
C	200	1.69	0.02	0.097	0.007	-0.31	0.6
C	200	1.98	0.03	0.128	0.011	-0.42	1.2
A	200	0.25	$2 \cdot 10^{-5}$	0.020	$3 \cdot 10^{-7}$	-0.22	4.5

parison with IPA (see Table III), is reflected in lower values of both κ and ρ (Table VI).

In many practical systems, TPA is completely esterified by an excess of glycol in a first stage, after which an excess of IPA is added to convert these OH-functional prepolymers into COOH-functional resins. As a consequence, the final extent of the reaction of IPA is usually close to 50%, which means that the simple model 1 can be applied for these systems. Yet, it should be borne in mind that the reaction kinetics in such a practical system might still be different from the kinetics studied with these model reactions. However, we think that this is the best approximation possible to date.

CONCLUSIONS

Below $\alpha = 0.6$, the kinetics of the heterogeneous reaction of IPA with BA can be well described with a simple kinetic model for a homogeneous reaction, with only a positive substitution effect in IPA. For the reaction of TPA with BA, an acceptable description holds for the full range of conversion. A more sophisticated model, in which insoluble particles and a surface reaction (and a substitution effect) are incorporated, yields a better description of the experiments. The model parameters are strongly dependent on temperature and the type of phthalic acid, which indicates that the heterogeneity of the reaction mixture is the main cause of the kinetic effects observed.

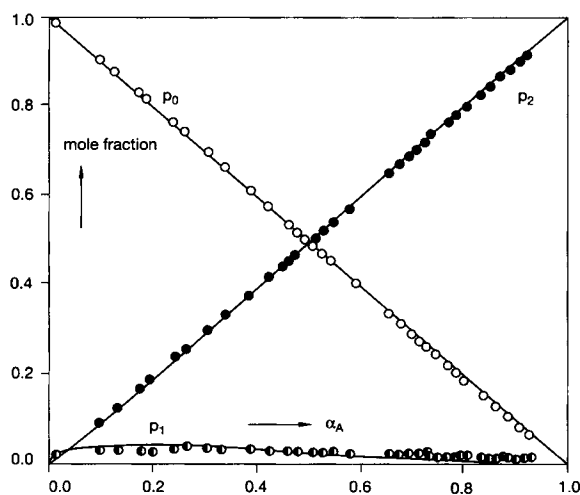


Figure 7 Experimental and fitted reaction states of TPA at 200°C (model 2). Curve calculated with $\kappa = 0.25$ and $\rho = 0.020$.

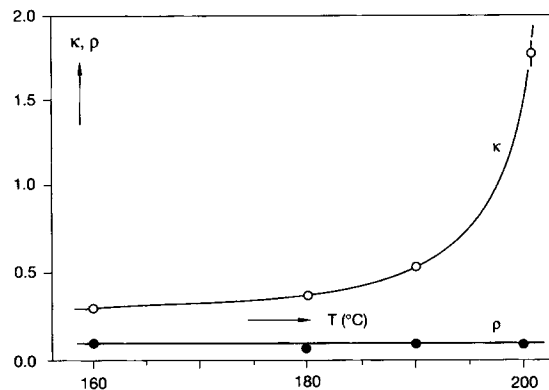


Figure 8 Surface effect parameters of IPA as functions of temperature (model 2).

The authors wish to thank Ir. M. J. A. T. Huijben-Backhuijs for mathematical assistance and for performing the regression analysis, Mrs. T. Schwarz and Mr. H. Schell for performing the kinetic experiments during their stay at DSM Research, Mr. Y. Mengerink and Dr. S. v.d. Wal for their assistance with the HPLC analysis, and Ir. G. P. J. M. Tiemersma-Thoone, prof. M. Gordon, and Dr. K. Dusek for stimulating discussions.

APPENDIX A: DESCRIPTION OF MODELS 1 AND 2

Differential equations are only presented here for A (=TPA) and are derived as a function of the conversion, α .

Model 1

In model 1, the chemical kinetics are derived by a set of differential equations for a homogeneous system: all components are considered as being dissolved completely. Partial solubility of monomer A is thus only taken into account in the substitution effect K . Concentrations presented here are related to the total amounts of the components of interest:

$$\frac{dp_B}{d\alpha} = \frac{-2[A]_0}{[B]_0} \quad (\text{A1})$$

$$\frac{dp_0}{d\alpha} = \frac{-4p_0}{2p_0 + Kp_1} \quad (\text{A2})$$

$$\frac{dp_1}{d\alpha} = \frac{2(2p_0 - Kp_1)}{2p_0 + Kp_1} \quad (\text{A3})$$

$$\frac{dp_2}{d\alpha} = \frac{2Kp_1}{2p_0 + Kp_1} \quad (\text{A4})$$

in which $[A]_0$ and $[B]_0$ are concentrations at $\alpha = 0.0$ and p_B is the fraction of B, which is unreacted. Boundary conditions at $\alpha = 0.0$ are: $p_B = p_0 = 1.0$, and $p_1 = p_2 = 0.0$.

Model 2

In model 2, the phthalic acid is considered to be completely insoluble. The esterification reaction with benzylalcohol, leading to a monoester [first reaction as given in reaction (1)], occurs only at the surface of spherically shaped particles (of phthalic acid). The reactive fraction of unreacted phthalic acid (p_0^r) is thus only located at the surface of the particles and it reacts with a reaction rate constant k_1 . The once esterified product is assumed to be completely soluble in the liquid phase. By dissolution of this product, the surface of the particles is renewed (and the particle radius is decreased) with a surface renewal rate constant k_s , with $\kappa = k_s/k_1$.

At the beginning of the reaction, the surface to core ratio, ρ , of the phthalic acid, is defined as $\rho = p_0^r/p_0^u$, with p_0^u being the unreactive fraction in the core of the phthalic acid particles.

The change in p_0^r , as a function of conversion, is derived from the evolution of the surface to core ratio of the particles as a function of particle volume.

In practice, the solubilities are not zero; p_0^r and ρ thus contain both the reactive fraction at the surfaces of the undissolved crystals and the fraction phthalic acid dissolved in the melt. The relevant differential equations are:

$$\frac{dp_B}{d\alpha} = \frac{-2[A]_0}{[B]_0} \quad (\text{A1})$$

$$\frac{dp_0^r}{d\alpha} = \frac{-4p_0^r}{2p_0^r + Kp_1}$$

$$+ \frac{2p_0^u \kappa \left\{ 1 - \frac{[B]_0}{2[A]_0} (1 - p_B) \right\}^{2/3}}{[B]_0 p_B (2p_0^r + Kp_1)} \quad (\text{A5})$$

$$\frac{dp_0^u}{d\alpha} = \frac{-2p_0^u \kappa \left\{ 1 - \frac{[B]_0}{2[A]_0} (1 - p_B) \right\}^{2/3}}{[B]_0 p_B (2p_0^r + Kp_1)} \quad (\text{A6})$$

$$\frac{dp_1}{d\alpha} = \frac{2(2p_0^r - Kp_1)}{2p_0^r + Kp_1} \quad (\text{A7})$$

$$\frac{dp_2}{d\alpha} = \frac{2Kp_1}{2p_0^r + Kp_1} \quad (\text{A8})$$

in which $[A]_0$ and $[B]_0$ are concentrations at α

$= 0.0$ and p_B is the fraction of B that is unreacted. Boundary conditions at $\alpha = 0.0$ are: $p_B = p_0 = 1.0$ and $p_1 = p_2 = 0.0$. The reaction states p_0^r and p_0^u stand for reactive and unreactive fractions of p_0 , respectively, and are determined by:

$$p_0^r + p_0^u = p_0 \quad (\text{A9})$$

with boundary conditions at $\alpha = 0.0$:

$$p_0^r = \frac{\rho}{1 + \rho} \quad (\text{A10})$$

$$p_0^u = \frac{1}{1 + \rho} \quad (\text{A11})$$

APPENDIX B: DETERMINATION OF REACTION STATES FROM HPLC DATA

The determination of the reaction states are here only described for A. Initial concentrations are: $[A]_0$ and $[B]_0$. HPLC analysis results in the ratios $[AB]/[B]$ and $[AB_2]/[AB]$. A material balance in B then leads to:

$$[B] \left\{ 1 + \frac{[AB]}{[B]} + 2 \frac{[AB_2]}{[B]} \right\} = [B]_0 \quad (\text{B1})$$

which yields the value for $[B]$. From this value, the values for $[AB]$ and $[AB_2]$ are calculated. The reaction states are finally calculated with:

$$p_1 = \frac{[AB]}{[A]_0}, \quad (\text{B2})$$

$$p_2 = \frac{[AB_2]}{[A]_0} \quad (\text{B3})$$

and

$$p_0 = 1 - p_1 - p_2. \quad (\text{B4})$$

REFERENCES

1. P. J. Flory, *J. Amer. Chem. Soc.*, **58**, 1877 (1936); **63**, 3083, 3091, 3096 (1941); **69**, 30 (1947).
2. P. J. Flory, *Chem. Revs.*, **39**, 137 (1946).
3. P. J. Flory, *Principles of Polymer Chemistry*, Cornell University, Ithaca, NY, 1953.
4. W. H. Stockmayer, *J. Chem. Phys.*, **11**, 45 (1943); **12**, 125 (1944); *J. Polym. Sci.*, **9**, 69 (1952); **11**, 424 (1954).

5. M. Gordon, *Proc. Roy. Soc. A*, **268**, 240 (1962).
6. M. Gordon and G. R. Scantlebury, *Trans. Faraday Soc.*, **60**, 604 (1964); *Proc. Roy. Soc. A*, **292**, 380 (1966).
7. M. Gordon and G. R. Scantlebury, *J. Chem. Soc.*, **B**, 1 (1967).
8. M. Gordon and C. G. Leonis, *J. Chem. Soc. Faraday Trans. I*, **71**, 161, 178 (1975).
9. G. P. J. M. Tiemersma-Thoone, B. J. R. Scholtens, and K. Dusek, *Proceedings 1st International Conf. on Industrial and Applied Mathematics (ICIAM 87)*, Contributions from the Netherlands, A. H. P. van der Burgh and R. W. W. Mattheij, Eds., CWI Track 36, Amsterdam, 1987, p. 295.
10. G. P. J. M. Tiemersma-Thoone, B. J. R. Scholtens, K. Dusek, and M. Gordon, *J. Polym. Sci. Part B Polym. Phys.*, **29**, 463 (1991).
11. B. J. R. Scholtens and G. P. J. M. Tiemersma-Thoone, *Polym. Mater. Sci. Eng.*, **67**, 225 (1992).
12. J. L. McCarthy and B. J. R. Scholtens, *J. Appl. Polym. Sci.*, **42**, 2223 (1991).

Received April 5, 1993

Accepted June 1, 1993